ISSN 1560-3547, Regular and Chaotic Dynamics, 2020, Vol. 25, No. 2, pp. 199–214. © Pleiades Publishing, Ltd., 2020.

Simple Flows on Tori with Uncommon Chaos

Carles Simó*

Departament de Matemàtiques i Informàtica,
Universitat de Barcelona, BGSMath,
Gran Via 585, 08007, Barcelona, Catalonia

Received January 07, 2020; revised February 27, 2020; accepted March 02, 2020

Abstract—We consider a family of simple flows in tori that display chaotic behavior in a wide sense. But these flows do not have homoclinic nor heteroclinic orbits. They have only a fixed point which is of parabolic type. However, the dynamics returns infinitely many times near the fixed point due to quasi-periodicity. A preliminary example is given for maps introduced in a paper containing many examples of strange attractors in [6]. Recently, a family of maps similar to the flows considered here was studied in [9]. In the present paper we consider the case of 2D tori and the extension to tori of arbitrary finite dimension. Some other facts about exceptional frequencies and behavior around parabolic fixed points are also included.

MSC2010 numbers: 37C55, 37E35, 39A33
DOI: 10.1134/S1560354720020057

Keywords: chaos without homoclinic/heteroclinic points, chaotic flows on tori, the returning role of quasi-periodicity, zero maximal Lyapunov exponents, the role of parabolic points, exceptional frequencies

Dedicated to Prof. Valery Vasilievich Kozlov on the occasion of his 70th birthday

1. INTRODUCTION

Professor Kozlov is widely known for a large number of excellent publications on topics like mechanics of particles and systems, global analysis, analysis on manifolds, dynamical systems and ergodic theory, statistical mechanics, structure of matter, etc. These hundreds of publications, in which he had around 100 coauthors, are being largely cited along the years.

In one of his papers [8], at the beginning of the journal, he considered a charged particle in $\mathbb{T}^2$ under the action of a constant direction magnetic field. Later, when the field cancels but a lattice of atoms exists in the torus, it is shown that the dynamics of the charged particle is chaotic.

In the present work we consider a flow in the torus with a constant direction, satisfying nonresonance conditions. Only a parabolic fixed point exists at the origin but no homoclinic nor heteroclinic orbits exist. However, the dynamics turns out to be chaotic. The present paper extends to flows, in a more general context, some models for maps introduced in [9]. These models for maps could be seen as a detailed study of one of the examples introduced in the prologue of the proceedings of a conference in 1982, [6].

There are many different definitions of chaos, see, e. g., [1, 4, 12] and references therein. Poincaré [11] knew about the existence and relevance of chaos a long time ago. And E. Lorenz said about chaos "*When the present determines the future, but the approximate present does not approximately determine the future*", see [3].

In what follows we consider a flow defined on a torus, $\mathbb{T}^2$ first and $\mathbb{T}^n$ later. We denote the flow time t as φ_t. We shall consider that the dynamics is chaotic if it has

- Sensitive dependence on initial conditions (SDIC): A point x is said to have SDIC if there exists a fixed $\alpha > 0$ such that for every $\varepsilon > 0$ there exists a point y in the ball $B_\varepsilon(x)$ and a value $t = t(\varepsilon, x, y) > 0$ such that $d(\varphi_t(y), \varphi_t(x)) \geqslant \alpha$, where d denotes the distance. This implies lack of predictability. We shall require SDIC for a set of x of full measure.

*E-mail: carles@maia.ub.es

- Topological transitivity (TT): A flow is said to be TT if for every couple of open sets $\mathcal{A}, \mathcal{B}$ in the domain of definition of the flow there exists a $t > 0$ such that $\varphi_t(\mathcal{A}) \cap \mathcal{B} \neq \emptyset$.

We remark that SDIC appears in very simple, even Hamiltonian integrable systems. Kepler's problem is an example. But it misses the TT condition. A flow on a torus with a constant vector field whose components are nonresonant satisfies the TT condition, but it misses the SDIC condition.

In Section 2 we introduce the models that we consider first in $\mathbb{T}^2$ and then in $\mathbb{T}^n$. They mainly depend of a parameter $\gamma \geqslant 1$ which is responsible for the existence of a parabolic fixed point, giving rise to stable and unstable branches. The exceptional value $\gamma = 1$ is also considered. Initially we present very easy models and then we comment on modifications, adding some higher-order terms. In Section 3 we proceed to the study of the Lyapunov exponents, in tori of dimension $n \geqslant 2$, but excluding the case $\gamma = 1$. It is proved that in all cases the maximal Lyapunov exponent is zero. Then, in Section 4 we consider the exceptional case $\gamma = 1$ for nonresonant frequencies, and show anomalous behavior for some exceptional class of frequencies, the so-called ultra-Liouville ones. In Section 5 we look at some other examples of maps whose fixed points are parabolic. In Section 6 we present some conclusions.

2. THE MODEL

We shall consider $\mathbb{T}^2$ as the square $Q = [-1/2, 1/2] \times [-1/2, 1/2]$ identifying the opposite boundaries of Q. In a similar way we consider $\mathbb{T}^n$ as $[-1/2, 1/2]^n$.

Let $\omega \in (0, 1)$ be an irrational number and consider in $\mathbb{T}^2$ the ODE

$$\begin{pmatrix} dx/dt \\ dy/dt \end{pmatrix} = \begin{pmatrix} \omega f_\gamma(x, y) \\ f_\gamma(x, y) \end{pmatrix}, \qquad f_\gamma(x, y) = f(x, y)^{\gamma/2}, \qquad f(x, y) = \sin^2(\pi x) + \sin^2(\pi y), \quad (2.1)$$

and $\gamma \in \mathbb{R}$ with $\gamma \geqslant 1$. It is suitable, for the generalization to dimension n, that instead of the vector $(\omega, 1)^T$ as multipliers of f_γ in (2.1) we use a normalized vector $(\omega_1, \omega_2)^T = (\omega, 1)^T/\sqrt{1 + \omega^2}$.

This can be easily generalized to $\mathbb{T}^n$. To this end we consider a normalized vector $\Omega = (\omega_1, \omega_2, \ldots, \omega_n)^T$ such that the components are positive, they satisfy a nonresonance condition ($(\mathbf{k}, \Omega) \neq 0$ for all $\mathbf{k} \in \mathbb{Z}^n \setminus 0$) and, for concreteness, we assume $\omega_i < \omega_j$ if $i < j$. Let $\mathbf{x} = (x_1, \ldots, x_n)^T$ be the variables in $\mathbb{T}^n$. The differential equations are

$$d\mathbf{x}/dt = \Omega f_\gamma(\mathbf{x}), \quad i = 1, \ldots, n, \quad (2.2)$$

that is, $dx_i/dt = \omega_i f_\gamma(\mathbf{x})$, $i = 1, \ldots, n$, where, as before, $f_\gamma(\mathbf{x}) = f(\mathbf{x})^{\gamma/2}$ with $f(\mathbf{x}) = \sum_{i=1}^n f_i(x_i)$ and $f_i(x_i) = \sin^2(\pi x_i)$. Later, when looking for the Lyapunov exponents, we shall use the derivatives of f with respect to the x_i variables. These will be odd functions in $\mathbb{T}^n$ and the effects on the Lyapunov exponent will mostly cancel because of the antisymmetry. This could suggest changing the contributions of the form $\sin^2(\pi x_i)$ by adding some higher-order terms, keeping the period 1 and such that the derivatives have some even part. For instance, one can include terms of the form $\hat{\beta} \sin^3(\pi x_i) \cos(\pi x_i)$ with moderate values of $\hat{\beta}$). In this way the contributions of $f_i(x_i)$ satisfy $f_i(x_i) = (\pi x_i)^2(1 + \mathcal{O}(x_i))$. For simplicity we will assume that the functions f_i are analytical, so that the only possible loss of differentiability will come from the value of γ.

However, even not taking into account these possible cancellations, one can prove the results for the Lyapunov exponent without the need to take into account the changes of sign. That is, assuming all contributions to be positive. In the discrete 2D case, in the form $(x, y)^T \mapsto (x + \varepsilon\omega f_\gamma(x, y), y + \varepsilon f_\gamma(x, y))i^T$, using different values of γ, moderate values of ε (say 10^{-2} or 10^{-3}), several values of ω and thousands of initial conditions, the evidence is that the numerical estimates of the Lyapunov exponents are below 10^{-9}, see [9]. Note that, as remarked in this reference, for the discrete map there is no exact symmetry. If a point $P = (x, y)$ has $P^* = (x^*, y^*)$ as image, the symmetric $(-x^*, -y^*)$ of P^* do not has $(-x, -y)$ as image.

In the function $f(\mathbf{x})$ one can assume that the role of all the x_i is similar or it is different. It will be enough to assume period 1 in all the variables and that it satisfies $f(\mathbf{x}) = \pi^2||\mathbf{x}||^2(1 + \mathcal{O}(||\mathbf{x}||))$

for all $\mathbf{x} \in \mathbb{T}^n$, where the term $\mathcal{O}(||\mathbf{x}||)$ has a size bounded in absolute value by some $\beta < 1$ not close to 1. If in some expression one uses a value of $\mathbf{x}$ outside $\mathbb{T}^n$, it has to be reduced to $\mathbb{T}^n$ modulus 1 before looking for the bound.

It is convenient to introduce variables that make the model simpler. To this end in $\mathbb{T}^2$ we introduce the vector $\mathbf{V} = (\omega_1, \omega_2)^T$ and the vector $\mathbf{U} = (\omega_2, -\omega_1)^T$, also unitary and orthogonal to $\mathbf{V}$. We denote the coordinates as u and v using these two vectors as a basis, and have $x^2 + y^2 = u^2 + v^2$. The equations become

$$du/dt = 0, \quad dv/dt = f_\gamma(\omega_2 u + \omega_1 v, -\omega_1 u + \omega_2 v). \tag{2.3}$$

Figure 1 shows Q and the lines in the directions of $\mathbf{U}$ and $\mathbf{V}$. As a basic domain, instead of $[-1/2, 1/2]^2$ we can use the one bounded by E, F, G and H, equivalent to Q modulus 1. The segment bounded by E and H is obtained by moving the segment $x \in [-1/2, 1/2]$, $y = 0$ in the direction of $\mathbf{V}$ until it reaches $y = -1/2$. In a similar way the segment bounded by F and G is obtained when we reach $y = 1/2$.

The variable u moves between A and B, the line where $v = 0$. On the line bounded by C and D one has $u = 0$. Note that if, starting at some $u_0 = 0$, $v = 0$ and moving in the direction of $\mathbf{V}$, one reaches a point between F and G of coordinates $x, y = 1/2$, it should be identified with $x, y = -1/2$, and if x is to the right of H it should be shifted to $x - 1$. We can denote this domain as $\mathcal{D}_2$.

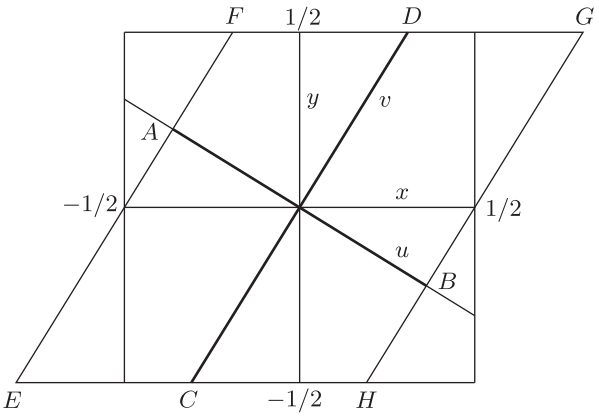

Fig. 1. The basic domains in the coordinates (x, y) and (u, v). See the text for details.

This can be generalized to $\mathbb{T}^n$ by constructing a domain to be denoted as $\mathcal{D}_n$. We select the vector Ω as $\mathbf{V}$ and should define the vectors $\mathbf{U}_i$, $i = 1, \ldots, n-1$, so that $\mathbf{U}_1, \ldots, \mathbf{U}_{n-1}, \mathbf{V}$ form an orthonormal basis. Let us denote the coordinates in this basis as $\mathbf{u}, v$, where $\mathbf{u} = (u_1, \ldots, u_{n-1})$.

We want to construct the vectors $\mathbf{U}_i$ in an easy way. Equivalently, we look for an $n \times n$ matrix A, with entries $a_{i,j}$, to pass from the $\mathbf{u}, v$ to the $\mathbf{x}$ coordinates. We take Ω as the last column in A: $a_{i,n} = \omega_i$, $i = 1, \ldots, n$. In principle one can take random vectors for the first $n-1$ columns and use Gram–Schmidt orthonormalization. Instead, we shall use another method with a cost $\mathcal{O}(n^2)$ and producing a simpler A.

First, for $i = 1, \ldots, n$ and $j = i, \ldots, n-1$ we copy $a_{i,j} = a_{i,n}$. Then for $j = 1, \ldots, n-1$ we define $a_{j+1,j} = -\sum_{i=1}^{j} a_{i,n}^2 / a_{j+1,n}$. The elements $a_{i,j}$, $i \geqslant 3$, $j = 1, \ldots, i-2$ are zero. Finally, we proceed to normalize the first $n-1$ columns.

For $j = 1, \ldots, n-1$ the vector $\mathbf{U}_j$ has the first $j+1$ entries different from zero (the first j ones are > 0 and the $j+1$ one is < 0) and the next ones are zero. To pass from $\mathbf{x}$ to the $\mathbf{u}, v$ coordinates, we use A^T and $||\mathbf{x}||^2 = ||\mathbf{u}||^2 + v^2$. Then Eq. (2.2) becomes

$$d\mathbf{u}/dt = 0, \quad dv/dt = f_\gamma, \tag{2.4}$$

where we recall that $f_\gamma = f^{\gamma/2}$ and $f = \pi^2(||\mathbf{u}||^2 + v^2)(1 + \mathcal{O}((||\mathbf{u}||^2 + v^2)^{1/2}))$. It is clear that $\mathbf{u} = 0, v = 0$ is the only fixed point in $\mathbb{T}^n$ and for $\gamma > 1$ the differential of the vector field in (2.4)

is zero at the fixed point. The point is parabolic, and if we fix $\mathbf{u} = 0$, the dominant term in the dynamics of v is $(\pi|v|)^\gamma$. As we shall see in Section 3, this allows us to study easily the passages near the origin.

The case $\gamma = 1$ is exceptional. Still, the origin is fixed, but for $v > 0$ it behaves like $\pi v(1 + \mathcal{O}(v))$, while for $v < 0$ it behaves like $-\pi v(1 + \mathcal{O}(v))$. Anyway, looking at the dynamics on $\mathbf{u} = 0$ or nearby, it has much in common with the case $\gamma > 1$, except for what concerns the time dependence. For $\gamma = 1$ we can say that the point is dynamically parabolic. See Section 5 for additional comments and examples of different parabolic points.

The points in $\mathbf{u} = 0$ with $v \in \mathbb{R}$, returning to $\mathbb{T}^n$ and taking the x coordinates modulus 1, are dense due to the nonresonance condition on Ω (see the next subsection). The ones with $v > 0$ form the unstable branch of the origin, to be denoted as W^u, and the ones with $v < 0$ form the stable branch W^s. We can denote them as $v^{u,s}(t)$ to make explicit the dependence in t. For instance, one can take $v^u(0) = 1/2$ for W^u and then $\lim_{t\to-\infty} v^u(t) = 0$, and $v^s(0) = -1/2$ for W^s and then $\lim_{t\to+\infty} v^s(t) = 0$. For any $t^* \in \mathbb{R}$ one has that the part $\{v^u(t), t \geqslant t^*\}$ of W^u is also dense, and similar for W^s.

The larger γ, the slower is the dynamics in the vicinity of the origin. This implies that the flow spends much more time near it. See Section 3.1 for details. And see also Section 2.2, Figs. 2, 4 and 5 and Table 1 in [9] for several statistical properties in the discrete case.

2.1. Chaoticity

Starting at a point with $x_n = 0$, we return to $x_n = 0$ and the values of the other $\mathbf{X}$ shift as $x_i \to x_i + \omega_i/\omega_n$ modulus 1, for $i = 1, \ldots, n-1$. Thanks to H. Weyl's theorem the values of the coordinates $x_i, i = 1, \ldots, n-1$ in the successive intersections tend to be equidistributed because $\omega_i/\omega_n\, i = 1, \ldots, n-1$ are also nonresonant. In particular, they are dense, and this implies the density of all the orbits when we consider $t \in \mathbb{R}$. The projections of the points in $x_n = 0$ in the $\mathbf{V}$ direction give also density and tendency to equidistribution of the $\mathbf{u}$ coordinates in $v = 0$.

Here one proves that the flows that we consider satisfy the chaoticity conditions. The key points are identical to the ones in [9] for maps.

Theorem 1. *The flow defined by* (2.2) *with* Ω *nonresonant satisfies the SDIC and TT conditions for chaoticity.*

Proof. Let P_1 be an arbitrary point in $\mathbb{T}^n$. Assume $P_1 \notin W^s$. As W^s is dense, for any $\varepsilon > 0$ there exists $P_2 \in W^s$ such that $d(P_1, P_2) < \varepsilon$. But when $t \to \infty$ one has $\varphi_t(P_2) \to 0$, while there are infinite values of t such that the x_n coordinate of $\varphi_t(P_1)$ reaches the value 1/2. Hence, the SDIC condition is satisfied for any $\alpha \leqslant 1/2$.

If $P_1 \in W^s$, it is enough to exchange the roles of P_1 and P_2. Furthermore, the SDIC condition is satisfied by all the points in $\mathbb{T}^n$.

Now consider two arbitrary open sets $\mathcal{A}$ and $\mathcal{B}$. Due to the density of W^u there are points in $\mathcal{A}$ which belong to W^u. Let t^* be the time parameter in W^u of one of these points. As the points in W^u with parameter $t > t^*$ are also dense, there exist values $t^{**} > t^*$ such that the point in W^u with parameter t^{**} belongs to $\mathcal{B}$. Hence, $\varphi_{t^{**}-t^*}(\mathcal{A}) \cap \mathcal{B} \neq \emptyset$. □

3. BOUNDING THE MAXIMAL LYAPUNOV EXPONENT FOR $\gamma > 1$

As is well known for a flow φ_t and an initial point located at $\mathbf{p}_0$ for $t = 0$, one should look for the maximal value, for all vectors $\mathbf{w}_0$, (one can assume $||\mathbf{w}_0|| = 1$), of the limit

$$\Lambda = \limsup_{t\to\infty} \frac{1}{t} \log\left(||D\varphi_t(\mathbf{p}_0)\mathbf{w}_0||\right), \tag{3.1}$$

where $D\varphi_t$ denotes the differential of the flow with respect to the initial conditions, that is, the first-order variational equations. It is clear that the value of Λ is the same for all points in the orbit

of $\mathbf{p}_0$. Let us denote as M the matrix $D\varphi_t$ of the variational equations. In the present case, using the variables in (2.4) it satisfies the equation

$$\frac{dM}{dt} = \begin{pmatrix} 0 & 0 & \dots & 0 & 0 \\ 0 & 0 & \dots & 0 & 0 \\ \dots & \dots & \dots & \dots & \dots \\ \frac{\partial f_\gamma}{\partial u_1} & \frac{\partial f_\gamma}{\partial u_2} & \dots & \frac{\partial f_\gamma}{\partial u_{n-1}} & \frac{\partial f_\gamma}{\partial v} \end{pmatrix} M, \tag{3.2}$$

where the first $n-1$ rows of the differential matrix are zero, as follows from (2.4), and one has $M(0) = Id$. Due to the form of (3.2) one has $m_{i,i}(t) = 1$ for $i = 1, \dots, n-1$ and $m_{i,j}(t) = 0$ for $i = 1, \dots, n-1$, $j \neq i$, for all t. Only the elements $m_{n,j}$, $j = 1, \dots, n$ change with time.

The domain $\mathcal{D}_n$ in which the coordinates $\mathbf{u}$ and v move in $\mathbb{T}^n$ is a generalization of the one displayed in Fig. 1. Instead of the segment on $y = 0$ in which $x \in [-1/2, 1/2]$ now we have the hyperplane $x_n = 0$ with $(x_1, \dots, x_{n-1})$ moving in the hypercube $\hat{Q} = [-1/2, 1/2]^{n-1}$. The full domain, that in the case $n = 2$ is bounded by the points E, F, G and H, is bounded in the upper part of $\mathbb{T}^n$ by moving $\hat{Q}$ in the direction of $\mathbf{V}$ until it reaches $x_n = 1/2$ and in the lower part until it reaches $x_n = -1/2$. We can denote these upper and lower bounds of the domain as $\hat{Q}_u$ and $\hat{Q}_l$. Instead of the segment of u between A and B one has a parallelogram, which we denote as $\mathcal{P}_{n-1}$, obtained as the projection of $\hat{Q}$ in the direction of $\mathbf{V}$ until it reaches the hyperplane generated by the vectors $\mathbf{U}_1, \dots, \mathbf{U}_{n-1}$.

We also note that in Fig. 1 the values of u between A and B are bounded by a value which depends on the direction of $\mathbf{V}$. The bound of $|u|$ takes values between $1/2$ and $(1/2)/\sqrt{2}$. But the value $1/2$ is inadmissible, because this would mean that $\omega_1 = 0$. One can check that in dimension n, inside $\mathcal{P}_{n-1}$, there is a sphere, to be denoted as $\mathcal{S}_{n-1}$, whose radius $||\mathbf{u}||$, using the Euclidean norm, has the same bounds. As in the case $n = 2$, the value $1/2$ is inadmissible. However, it is clear that, depending on $\mathbf{V}$, one can have points in $\mathcal{P}_{n-1}$, located at the boundary, with $||u|| = \sqrt{n-1}/2$.

For simplicity let us denote as f_{u_i} the derivatives $\frac{\partial f_\gamma}{\partial u_i}$ for $i = 1, \dots, n-1$ and as f_v the last one, $\frac{\partial f_\gamma}{\partial v}$. In a similar way we shall denote f_γ as f, but in all cases we keep in mind that this f depends on γ. Then the relevant part of (3.2) can be written as

$$\frac{dm_{n,i}}{dt} = f_{u_i} + f_v m_{n,i} \quad \text{for } i = 1, \dots, n-1, \qquad \frac{dm_{n,n}}{dt} = f_v m_{n,n}. \tag{3.3}$$

Letting aside the irrelevant values $m_{i,i} = 1$ for $i = 1, \dots, n-1$, it is clear that one can bound the norm of $M(t)$ as $\sum_{i=1}^{n} |m_{n,i}|$.

3.1. The Relevant Contributions to Λ

To have bounds for Λ one can consider a very large number of passages through $\mathcal{P}_{n-1}$, to have upper estimates of the norm of M and lower estimates of t and let the number of passages tend to $+\infty$.

We can assume that we start at some point in $\hat{Q}_l$, then we move in the direction of $\mathbf{V}$ until we reach $\hat{Q}_u$. In this motion the value of $\mathbf{u}$ is constant. Then we identify the final point with the corresponding one in $\hat{Q}_l$ taking the values of the x_i modulus 1. The process is repeated indefinitely.

Hence, we are crossing $\mathcal{P}_{n-1}$ at different values of $\mathbf{u}$. As mentioned above and according to Weyl's theorem, the crossings through $\hat{Q}$ tend to be equidistributed, and the same happens with the crossings of $\mathcal{P}_{n-1}$. We want to see the contributions of the different passages to the norm of M and to t.

Obviously, we shall not take the initial point in W^s. It turns out that it is more convenient to use v instead of t as an independent variable and to consider the change of t as a function of v. Then the equations in (2.4) and (3.3) become

$$\frac{dt}{dv}=\frac{1}{f},\qquad \frac{dm_{n,i}}{dv}=\frac{f_{u_i}}{f}+\frac{f_v}{f}m_{n,i}\ \text{ for } i=1,\dots,n-1,\qquad \frac{dm_{n,n}}{dv}=\frac{f_v}{f}m_{n,n},\tag{3.4}$$

beyond $d\mathbf{u}/dv=0$.

From the last equation in (3.4) it follows immediately that $m_{n,n}=cf$ for some constant c. As the equations for $m_{n,i}$, $i=1,\dots,n-1$ are linear and the homogeneous part coincides with the equation for $m_{n,n}$, we look for solutions of the form $m_{n,i}=g_i(v)f$ and obtain

$$\frac{dg_i}{dv}=\frac{f_{u_i}}{f^2}\ \text{ for } i=1,\dots,n-1.\tag{3.5}$$

We note that f in $\hat{Q}_u$ and $\hat{Q}_l$ has lower and upper bounds of the form $(\pi^2(1/2)^2(1-\beta))^{\gamma/2}$ (when only $|x_n|=1/2$ and the remaining x_i are zero) and $(\pi^2 n(1/2)^2(1+\beta))^{\gamma/2}$ (when $|x_n|=1/2$ and the remaining $|x_i|$ are also $1/2$). We recall that β is assumed to be a small value to bound the effect of extra terms. Therefore, the relevant part of the change of the norm of M going from $\hat{Q}_l$ to $\hat{Q}_u$ is $\sum_{i=1}^{n-1}\Delta g_i+1$ times a positive constant bounded from below and from above. In this last sum we put simply Δg_i to denote the change of this variable in the passage. As the constants we mentioned before do not play any relevant role in Λ, it is enough to concentrate on bounding the changes in the values of g_i, $i=1,\dots,n-1$ and t in a passage through $v=0$ for a given $\mathbf{u}$. In the case $n=2$ we refer simply to g instead of g_1.

In the next subsection we bound the values Δg_i, Δt for passages from $\hat{Q}_l$ to $\hat{Q}_u$ for a given value of $\mathbf{u}$. As it follows from (3.4) and (3.5), only some simple integrals must be evaluated.

3.2. Evaluation of the Required Integrals

We consider first the case $n=2$ and the effect of the terms which come from $(u^2+v^2)^{\gamma/2}$ in f_γ. Later we shall comment on the effect of the terms $\mathcal{O}(x)$ and in the cases $n>2$.

We look at the case $u>0$ and, in principle, we assume it to be small. The values obtained for $u<0$ can cancel the ones with $u>0$ due to antisymmetry. Then we could consider the effect of high-order symmetric terms, as mentioned at the beginning of Section 2, but it not necessary if we do not take into account the cancellations. It is not required to obtain the desired results.

We assume that we start from a value $u>0$ and $v=0$ until we reach the maximal value of v, say v_m, when $y=1/2$, see Fig. 1. The value v_m is of the order of $1/2$. In a similar way we can consider the passage from $v<0$ on $y=-1/2$ until we reach $v=0$ and just look at the absolute value of the contributions to the variation of g. In a similar way we look for the contributions to the variation of t.

Proposition 1. *The contribution to the variation of g of the terms $(u^2+v^2)^{\gamma/2}$ for $u>0$ is of the order of $u^{-\gamma}$ for $\gamma\geqslant 1$. The one for t is of the order of $u^{-(\gamma-1)}$ for $\gamma>1$ and of the order of $\log(1/u)$ for $\gamma=1$. The values for $\gamma=1$ will be used in the next section.*

Proof. As $dg/dv=\gamma u/(u^2+v^2)^{\gamma/2+1}$, it is suitable to introduce a new independent variable $z=v/u$ and, for $\gamma\geqslant 1$, one has the following approximation to the contribution of a given passage through some value of $u>0$ to the change in g:

$$\int_0^{v_m}\frac{u\,dv}{(u^2+v^2)^{\gamma/2+1}}=\int_0^{v_m/u}\frac{dz}{u^\gamma(1+z^2)^{\gamma/2+1}}\approx\frac{1}{u^\gamma}I_{\gamma+2},\tag{3.6}$$

where for $a>1$ we define $I_a=\int_0^\infty\frac{dz}{(1+z^2)^{a/2}}$. If u is small, the value $z_m=v_m/u$ is large, and the integral from 0 to z_m is close to $I_{\gamma+2}$. The contribution on the same u with $v<0$ is similar, but with negative sign. But, as mentioned above, we shall not consider these cancellations.

Now we proceed to compute the integrals which come from dt/dv : $\int_0^{v_m}dv(u^2+v^2)^{-\gamma/2}$ for small u. Due to the parity of the integrand, it is enough to have expressions for $u>0$ and in a range with $v\geqslant 0$. In contrast with the previous ones, one has to distinguish for $\gamma>1$ and $\gamma=1$.

- For $\gamma > 1$ and introducing again $z = v/u$ we have
$$\int_0^{v_m} \frac{dv}{(u^2+v^2)^{\gamma/2}} = \int_0^{v_m/u} \frac{dz}{u^{\gamma-1}(1+z^2)^{\gamma/2}} \approx \frac{1}{u^{\gamma-1}} I_\gamma. \tag{3.7}$$
- For $\gamma = 1$ we introduce the change $v = u\sinh(z)$, define z_m by $v_m = u\sinh(z_m)$ and obtain
$$\int_0^{v_m} \frac{dv}{(u^2+v^2)^{1/2}} = \int_0^{z_m} dz = z_m = \log(1/u) + \mathcal{O}(1). \tag{3.8}$$

Clearly, if $n > 2$ the contributions of the g_i have expressions like (3.6). □

Some remarks are relevant:

Remarks. Several comments are useful to help to bound the Lyapunov exponent. We list some of them.

- From (3.1) it is clear that to bound Λ we can use upper bounds of the numerator and lower bounds of the denominator. In the statement of Proposition 1 we do not include the upper bounds $I_{\gamma+2}$ which appear in (3.6). As will be clear in the next subsection, these constants are irrelevant in front of other arbitrary large contributions.
- The same thing happens for the lower bounds which should be included in the expression of the change in t. For very small u the integral in (3.7) is very close to I_γ, because v_m/u is very large, and the term $\mathcal{O}(1)$ in (3.7) is very small compared to the dominant term. For not so small values of u these contributions to the changes in t can be ignored because lower bounds are enough.
- To look for the total contributions of the passages through $\mathcal{P}_{n-1}$, one should integrate the contributions through a given u (using u as $||u||$ if $n > 2$). For upper bounds we can integrate on a sphere $\hat{\mathcal{S}}_{n-1}$ which contains $\mathcal{P}_{n-1}$ and for lower bounds we can use a sphere smaller than $\mathcal{S}_{n-1}$. To this end we should multiply the results in Proposition 1 by u^{n-2} and integrate between 0 and the radii of these spheres. The constant factors $A_m = 2\pi^{(m+1)/2}/\Gamma((m+1)/2)$ for the area element in dimension m, being in our case $m = n-2$, can be neglected as done before with other constants.
- As mentioned in Section 3.1, the increase in the norm of M contains the sum of the Δg_i plus 1. As we have in Proposition 1 the bound for one of the Δg_i and it is larger that 1, it is enough to bound by n times the value given in (3.6). As said for other constants, including this constant is also irrelevant.
- Higher-order terms in the numerator of the function to be integrated in (3.6) can come from higher-order terms in f, as mentioned in Section 2, to destroy antisymmetry. The addition of terms like $\sin^3(\pi x_i)\cos(\pi x_i)$ produces that near the origin instead of u in the numerator of (3.6) we can have u^2, uv or v^2. Similarly for the addition of other terms. The factors v can simply be bounded by a constant and do not affect essentially the value of the integral. The factors in u, or their absence, simply change the exponent $-\gamma$ of u in the final value.

3.3. The Bounds of the Exponent

The goal of this subsection is to prove

Theorem 2. *The flow defined by* (2.2) *with* Ω *nonresonant and* $\gamma > 1$ *has zero maximal Lyapunov exponent.*

Proof. It follows from Proposition 1 and the third of the previous comments that one of the things to do is to integrate $u^{-\gamma}$ and $u^{-\gamma+1}$ times u^{n-2} until a radius $r_{\max}$ which contains $\mathcal{P}_{n-1}$ in the first case and contains in $\mathcal{S}_{n-1}$ in the second one. In all cases it is of the order of 1. Concerning the inner radius we take a very small value r_0 to be specified later.

One has to evaluate the integrals from r_0 to $r_{\max}$ of $u^{m-2-\gamma}$ for the contributions to the norm of M and to t. In the integrals one has to include a density $\mathbf{D}$ which increases towards ∞ as $t \to \infty$. We note that the density tends to have the same value in the full domain (again by Weil's

theorem), but as r_0 can be rather small, the number of iterates inside the ball of radius r_0 can be quite different from the volume of the ball times $\mathbf{D}$. We shall see that this is not relevant.

Let $\kappa = -\gamma + n - 2$ be the exponent of u when we integrate terms coming from (3.6) and $\kappa = -\gamma + n - 1$ when we do the same with (3.7). Let us denote as J_κ the integral of u^κ from r_0 to $r_{\max} = \mathcal{O}(1)$. The integral is $\mathcal{O}(1)$, $\mathcal{O}(\log(1/r_0))$, $\mathcal{O}(r_0^{-\kappa-1})$ if $\kappa > -1$, $= -1$, < -1, respectively.

Given a value of r_0 to be specified, we consider the passages through $\mathcal{S}_{n-1}$ divided into two parts: the ones that have $u = ||\mathbf{u}|| \geqslant r_0$ and the ones with $u < r_0$. The contributions of the first ones to M and t can be estimated as $C_2 := J_{n-2-\gamma}\mathbf{D}$ and $C_4 := J_{n-1-\gamma}\mathbf{D}$, respectively. Let us denote as $u_k, k \in K = \{1, 2, \ldots, l\}$ the values of $u < r_0$, which we assume to be ordered: $u_1 \leqslant u_2 \leqslant \ldots \leqslant u_l$. The passages through these values of u_k give contributions (slipping irrelevant constants)

$$C_1 := \sum_{k=1}^{l} u_k^{-\gamma}, \qquad C_3 := \sum_{k=1}^{l} u_k^{-\gamma+1}. \tag{3.9}$$

Therefore, we should estimate $\frac{\log(C_1+C_2)}{C_3+C_4} < \frac{\log(C_1)+\log(C_2)}{C_3+C_4}$, taking into account that C_1 and C_2 are large. Given an arbitrary value of $\varepsilon > 0$, to prove that the ratio is less than ε it is enough to show that $\log(C_1)/C_3 < \varepsilon$ and $\log(C_2)/C_4 < \varepsilon$. Let us introduce $\delta_k = u_k/u_1 \geqslant 1$ for $k = 1, \ldots, l$. From (3.9) we can write

$$\log(C_1) = \log(u_1^{-\gamma}) + \log(a), \quad a = \sum_{k=1}^{l} \delta_k^{-\gamma}, \quad C_3 = u_1^{-\gamma+1} b, \quad b = \sum_{k=1}^{l} \delta_k^{-\gamma+1}. \tag{3.10}$$

It is clear that $1 \leqslant a \leqslant b$ and then $\log(a) < b$. If r_0 is small enough, one has $r_0^{\gamma-1} \leqslant \varepsilon/2$ and then $u_1^{\gamma-1} \leqslant \varepsilon/2$. Hence, $\log(a)/C_3 < \varepsilon/2$. Also, $\log(r_0^{-\gamma}) r_0^{\gamma-1}$ tends to zero and is decreasing if $r_0 < \exp(-1/(\gamma-1))$. Then $\log(r_0^{-\gamma})/C_3 < \varepsilon/2$ if r_0 is sufficiently small. It follows from (3.10) that $\log(C_1)/C_3 < \varepsilon$.

When r_0 has been fixed, the values of the constants $J_{n-2-\gamma}$, $J_{n-1-\gamma}$ are known. This allows one to use a value of $\mathbf{D}$ sufficiently large so that $\log(C_2)/C_4 < \varepsilon$. Note that $\mathbf{D} \to \infty$ when the number of passages through $\mathcal{S}_{n-1}$ tends to ∞. This completes the proof. □

4. SOME EXAMPLES OF THE BEHAVIOR OF THE MAXIMAL LYAPUNOV EXPONENT IN THE CASE $n = 2$ AND $\gamma = 1$

Here we shall consider some simple examples in dimension 2, concerning the limit case $\gamma = 1$. We shall see that for very exceptional values of ω one finds changes.

For simplicity we shall assume that we start in the invariant branch of the origin under (2.1). That is, in the successive passages through $y = 0$ the value of x increases by ω (taking mod 1 when $x \geqslant 1/2$). This implies increments of u by $\omega/\sqrt{1+\omega^2}$ to be denoted as $\bar{\omega}$. If we reach or exceed the point B in Fig. 1, we pass to A or to the right of A. Anyway we shall identify the successive passages through $y = 0$ by the value of x. The related value of u needed to apply the results in Proposition 1 is simply $\bar{\omega}x$.

This is not a too relevant assumption, because starting at any value of x we shall reach values arbitrarily close to 0 after a sufficiently large number of passages through $y = 0$.

For the quotient in (3.1) we shall assume that for the estimate of the norm of M we use the symmetric case without powers of u in the numerator of the integral in (3.6), as mentioned in the last item of Remarks 1. This means that in (3.6) the integral is $\mathcal{O}(u^{-2})$. The contribution to t keeps being $\log(1/u)$.

The basic idea is as follows: Assume we take a best approximant p/q of ω. Then $|\omega - p/q|$ is less than $1/q^2$. Perhaps much less if the next quotient in the CFE of ω is large compared to q. See, e. g., [7] as a basic reference and [5] for discussion and dynamical applications. Then the first $q-1$ iterates will be approximately equispaced in $[-1/2, -1/(2q)) \cup (1/(2q), 1/2]$ and the q iterate will be the closest one to 0. Then we can estimate the contributions to the norm of M and to t by integrating u^{-2} and $\log(1/u)$ in the ranges above and add the contribution of the iterate closest to 0.

Proposition 2. *Assume ω satisfies a Diophantine condition $|\omega - p/q| > c/q^\tau$, $c > 0, \tau \geqslant 2$ for all $q > 0$, $p/q \in \mathbb{Q} \setminus \{0\}$. Then the maximal Lyapunov exponent in the present models is zero. The same is true for the Liouville constant $\sum_{k=1}^{\infty} 10^{-k!}$.*

Proof. First we consider the case ω Diophantine. For the norm of M we approximate the contribution in $(1/(2q), 1/2]$ by the integral of u^{-2} times the density q and multiply by 2 to take into account the part of $u < 0$. Then we add the contribution of the last iterate, which satisfies the condition that the distance to the origin is $\approx c/q^{\tau-1}$. Skipping irrelevant constants, we obtain a bound

$$4q^2 + \frac{q^{2(\tau-1)}}{c^2}. \tag{4.1}$$

For t we obtain

$$q(1 + \log(2)) + \mathcal{O}(\log(q)/q) + \log\left(\frac{q^{\tau-1}}{c}\right). \tag{4.2}$$

Clearly the log of the expression in (4.1) divided by (4.2) tends to zero when $q \to \infty$.

For the Liouville constant we can use as q a value of the form $10^{m!}$ and then the distance to 0 of the q iterate is $\approx 10^{m!}/10^{(m+1)!}$. The main changes appear in the last term in (4.1), of the order of $(10^{(m+1)!}/10^{m!})^2$, and in the first term of (4.2) where q should be replaced by $10^{m!}$. Hence, the dominant terms for Λ are $2\log(10^{(m+1)!})/10^{m!}$, which clearly tends to zero as $m \to \infty$. □

Remark 1. As is well known, the set of Diophantine numbers with $\tau > 2$ has full measure. One can weak the condition to $|\omega - p/q| > c/(q^2(\log(q))^\tau)$, $c > 0$, $\tau > 1$, according to the Khinchin criterion to keep full measure. The Liouville constant is clearly non-Diophantine, but it is relevant as used by Liouville to show the existence of transcendental numbers.

As a curiosity we can consider some uncommon values of ω, like the so-called "ultra-Liouville" numbers. See, e. g., [10] and references therein. As an example let us define $\mathrm{tp}^{[0]}(x) = x$ and $\mathrm{tp}^{[m+1]}(x) = 2^{\mathrm{tp}^{[m]}(x)}$ for $m \geqslant 0$. Of course, instead of the basis 2 we can use another integer basis > 2.

We make a simple choice like

$$\omega = \sum_{k \geqslant 0} \frac{1}{\mathrm{tp}^{[k]}(2)} = \frac{1}{2} + \frac{1}{4} + \frac{1}{16} + \frac{1}{65536} + \frac{1}{2^{65536}} + \frac{1}{2^{2^{65536}}} + \ldots. \tag{4.3}$$

Proposition 3. *The maximal positive exponent if we use ω as in* (4.3) *is positive.*

Proof. We can look at best approximants p/q taking $q = \mathrm{tp}^{[m]}(2)$. The minimal distance to 0 will be $\approx \mathrm{tp}^{[m]}(2)/\mathrm{tp}^{[m+1]}(2)$. In $\sum_{i=1}^{p} u_i^{-2}$ the term which dominates comes from the passage at minimal distance: $(\mathrm{tp}^{[m+1]}(2)/\mathrm{tp}^{[m]}(2))^2$. In $\sum_{i=1}^{p} \log(1/u_i)$ both the term $(1 + \log(2))\mathrm{tp}^{[m]}(2)$, coming from the equidistributed constributions, and the final one, $\log(\mathrm{tp}^{[m+1]}(2)/\mathrm{tp}^{[m]}(2))$, are relevant. In both cases, as $\mathrm{tp}^{[m+1]}(2)$ is much larger than $\mathrm{tp}^{[m]}(2)$ and we take logarithms, the part which is dividing is negligible. Furthermore, $\log(\mathrm{tp}^{[m+1]}(2)) = \log(2)\mathrm{tp}^{[m]}(2)$.

Hence, using in the quotient in (3.1) the dominant terms in t and in the norm of M, we obtain

$$\frac{2\log(2)\mathrm{tp}^{[m]}(2)}{\log(2)\mathrm{tp}^{[m]}(2) + (1 + \log(2))\mathrm{tp}^{[m]}(2)}, \tag{4.4}$$

which gives the ratio $2\log(2)/(1 + 2\log(2))$. It is clear that, if we define $\mathrm{tp}^{[m]}(x)$ by replacing the basis 2 with any other integer basis > 2, we obtain a similar result. □

5. SOME MAPS WITH PARABOLIC FIXED POINTS AND POSITIVE LYAPUNOV EXPONENT

In the previous sections we have studied a model which has a parabolic point of a special type: it has an invariant manifold through the origin, which is the only fixed point, with one unstable branch and a stable one. We have shown that the Lyapunov exponent is zero in all cases for $\gamma > 1$.

In this section we want to consider a couple of examples (we shall use discrete 2D maps) to see the effect of more general parabolic fixed points, not leading to zero Lyapunov exponents.

To begin with, and considering always $x > 0$, $y > 0$, we recall that for a differential equation in the hyperbolic case, using as a simple model $x' = -\lambda x$, $y' = \lambda y$ with initial conditions $x(0) = 1$, $y(0) = y_0$, with $y_0 > 0$ very small, one has the following trivial facts: a) the time to reach $y = 1$ is $t_f = \log(1/y_0)/\lambda$ and then $x(t_f) = y_0$; the product xy is a first integral; c) the minimal distance to the origin occurs when $x = y = \sqrt{y_0}$; d) if in the expression of the Lyapunov maximal exponent we look at the quotient when $t = t_f$, instead of going to $+\infty$, we obtain λ.

We note that letting t go to $+\infty$ can produce a cancellation of this last value, as it happens if we start inside an homoclinic loop to the fixed point in a conservative integrable system.

Now we consider parabolic cases with equations $x' = -x^\gamma$, $y' = y^\gamma$, where $\gamma > 1$. We can look at similar properties, and with elementary computations we obtain the following

Proposition 4. *In the passage near a parabolic fixed point which is dynamically hyperbolic one has:*

- *The time to reach $y = 1$ is $t_f = (1/y_0^{\gamma-1} - 1)/(\gamma - 1)$ and then, as before, $x(t_f) = y_0$.*
- *One has the first integral $x^{-(\gamma-1)} + y^{-(\gamma-1)} = \text{constant} = 1 + y_0^{-(\gamma-1)}$.*
- *The minimal distance to the origin occurs when*

$$x = y = y_0 \left(\frac{2}{1 + y_0^{\gamma-1}} \right)^{1/(\gamma-1)} .$$

- *If we look at the contribution to the Lyapunov maximal exponent, but stopping at $t = t_f$ as before, we obtain*

$$\frac{\gamma \log(1/y_0)}{(y_0^{-(\gamma-1)} - 1)/(\gamma - 1)},$$

which tends to zero if $y_0 \to 0$. As noted in the hyperbolic case, it is the dynamics which appears for $t \to +\infty$ that gives the most important contribution to the Lyapunov exponent.

5.1. A Variant of the Standard Map

As a first example we consider a variant of the classical Chirikov standard map [2]. We can denote it as "cubical standard map" CSM. It is the composition of two triangular maps $CSM = F_2 F_1$ where

$$F_1 \begin{pmatrix} x \\ y \end{pmatrix} = \begin{pmatrix} x \\ y + \kappa \sin^3(x) \end{pmatrix}, \qquad F_2 \begin{pmatrix} x \\ y \end{pmatrix} = \begin{pmatrix} x + \sin^3(y) \\ y \end{pmatrix}, \tag{5.1}$$

κ being a real parameter that we shall consider positive. We assume $(x, y) \in \mathbb{T}^2$ and reduce mod 2π when required. The simple form as a composition of triangular maps allows us to obtain explicitly the inverse map.

The map has 4 fixed points: $(0, 0)$, (π, π), $(0, \pi)$ and $(\pi, 0)$. All of them are parabolic, the differential of CSM at them being the identity. The first two can be named parabolic topologically hyperbolic, because they have an unstable and a stable invariant manifold. The other two can be named limit elliptic parabolic points. Let us consider first these second points.

Let us shift the origin to $(0,\pi)$ with $u = x$, $v = y - \pi$. Near the fixed point the map can be approximated by the differential equation $u' = -v^3$, $v' = \kappa u^3$. This system has the first integral $I_e(u,v) = \kappa u^4 + v^4$. For this approximation the point $u = 0, v = 0$ is surrounded by invariant curves and most of them subsist for the discrete map. Assume that we start from a point $u = u_0 > 0$, $v = 0$. The orbit rotates counterclockwise. According to the first integral, it reaches $u = 0$ with $v = \kappa^{1/4} u_0$. An elementary computation shows that the period for the flow is

$$T = \frac{4}{\kappa^{3/4} u_0^2} J_3, \qquad J_3 = \int_0^1 \frac{dz}{(1-z^4)^{3/4}} \approx 1.8540746773. \tag{5.2}$$

Different checks for many values of κ and small values of u_0 show that using the map (5.1) gives evidence that one obtains invariant curves and that the number of iterates coincides with T with relative errors below 0.001. We note that the period (or the number of iterates) tends to ∞ as $u_0 \to 0$. This is the reason to name it a limit elliptic parabolic point. If we look around $(\pi, 0)$, the behavior is identical, but the rotation is clockwise.

Figure 2 shows an example, in (u,v) coordinates, using $\kappa = 0.0625$, $u_0 = 0.04$ on the left. For better visualization the values of (u,v) have been multiplied by 100. On the right side one can see the evolution of the first integral of the flow, $I_e(u,v)$, evaluated on the iterates of the map. The value for the flow is 1.6×10^{-7}. In the plot the values on the iterates have been multiplied by 10^6 for better visualization. One checks that the maximal differences have a relative value of 0.0005. The number of iterates to return very close to the initial point is 37105.

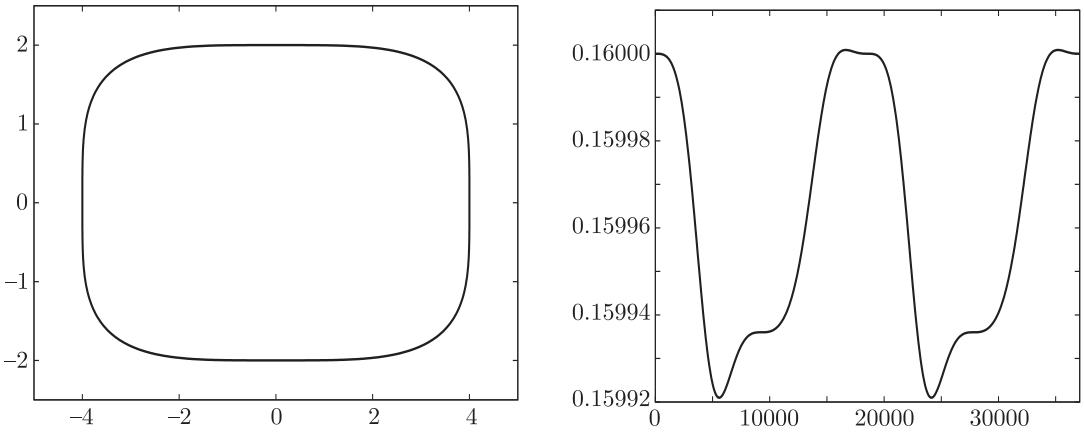

Fig. 2. Example of an approximate invariant curve of (5.1) around $(0,\pi)$. Left: the curve with the central point shifted to $(0,0)$. Right: evolution on the iterates of the map of the first integral of the approximation flow. See the text for details.

As a curious thing, if for this example of invariant curves around $(u,v) = (0,0)$ we replace the differential equations that we used by $u' = -\text{sign}(v)|v|^\gamma$, $v' = \kappa\,\text{sign}(u)|u|^\gamma$ with $\gamma > 1$, which for $\gamma = 3$ reduce to the equations that approximate (5.1), we obtain similar results, but the expression of the period becomes

$$T = \frac{4}{\kappa^{\gamma/(\gamma+1)} u_0^{\gamma-1}} J_\gamma, \qquad J_\gamma = \int_0^1 \frac{dz}{(1-z^{\gamma+1})^{\gamma/(\gamma+1)}} = \frac{\Gamma(1/(\gamma+1)^2}{(\gamma+1)\Gamma(2/(\gamma+1)}. \tag{5.3}$$

The value of J_γ is not relevant, because it increases monotonically from $\pi/2$ to 2 as γ increases from 1 to ∞. The relevant part of T is the factor $u_0^{-(\gamma-1)}$ which shows the behavior of the rotation number $\approx 2\pi/T$ of the invariant curves around the limit elliptic parabolic points as a function of the exponent $\gamma > 1$. For $\gamma = 1$ the value of T becomes $2\pi/\sqrt{\kappa}$, of course.

Next, we pass to the behavior around $(0,0)$. In that case the ODE approximation that we have is $x' = y^3$, $y' = \kappa x^3$ and the related first integral is $I_h(x,y) = \kappa x^4 - y^4$. Hence, the approximate

invariant manifolds are $y = \kappa^{1/4}x$ (unstable, W_0^u) and $y = -\kappa^{1/4}x$ (stable, W_0^s). Shifting (π, π) to the origin, one has similar results, but the roles of the manifolds are exchanged. One can use an approximation of W_0^u, taking simple representations of the form $y = \sum_{i\geqslant 3} \alpha_i x^i$ and asking for invariance, and compute a convenient number of iterates of a fundamental domain. The same can be done with W_π^s. Or, as it happens if we use $\kappa = 1$, one obtains W_π^s from W_0^u via the symmetry $S(x, y) = (\pi - y, \pi - x)$. This gives the evidence of heteroclinic orbits, as illustrated in Fig. 3. As we shall comment later, there are values of κ for which these heteroclinics points do not exist, but there are homoclinics to $(0, 0)$ and to (π, π).

Another fact that is easy to detect is the existence of periodic orbits in the chaotic zones created by homo/heteroclinic points. For instance, for $\kappa = 1$ one finds a hyperbolic periodic orbit of period 10 starting at $\approx (1.547515113214069, 0)$ or, in a symmetric way because $\kappa = 1$, at $\approx (0, 1.547515113214069)$.

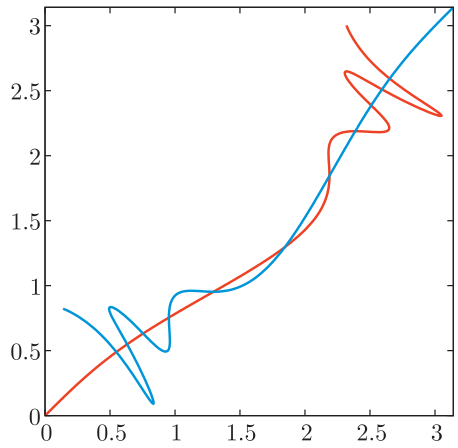

Fig. 3. The unstable invariant manifold of $(0, 0)$ (red) and the stable one of (π, π) (blue) for the map (5.1) and $\kappa = 1$, showing some heteroclinic points.

It is clear that if $\kappa = 0$, beyond the lines of fixed points $y = 0$ and $y = \pi$, and looking at what happens between them (the upper part is symmetric but moving from right to left) all the other lines $y = c$, for a constant $c \in (0, \pi)$, are invariant rotational curves (IRC) with rotation number $\rho = \sin^3(c)/(2\pi)$. The value of ρ increases for $c \in (0, \pi)$, has a maximum when $c = \pi/2$ and decreases again towards zero as $c \to \pi$.

Most of these IRC subsist when κ is small. These curves prevent the existence of heteroclinic points related to $(0, 0)$ and (π, π), but homoclinic points in $W_0^u \cap W_0^s$ and in $W_{\pi^u} \cap W_\pi^s$ certainly exist. They give rise to two chaotic zones which are disconnected because of the IRC.

When κ increases, due to the fact that the twist condition is satisfied except close to the maximum, many of the IRC subsist. But when κ is greater than $\kappa^* \approx 0.60763$, no IRC seem to exist, and the chaotic zones related to $(0, 0)$ and (π, π) are connected. But before κ^* there are some ranges of κ without IRC. The first one contains $\approx [0.5556, 0.5596]$. In particular, for $\kappa < \kappa_*$, $\kappa_* \approx 0.5555$ there is evidence of the existence of IRC. Other intervals before κ^* without IRC are approximately $[0.5845, 0.5860]$, $[0.5962, 0.5974]$, $[0.6022, 0.6030]$ and $[0.6057, 0.6063]$ plus some other very narrow intervals.

We can question how the IRC look like when κ is outside these excluded intervals but close to them. As a first example, Fig. 4 shows one of these curves for $\kappa = 0.56$, starting at $(0, 1.24)$. Other similar IRC can be found for nearby initial points.

The shape can seem strange, but it is natural. Indeed, as these curves are close to a maximum of ρ, one can lose the twist condition. Then non-Birkhoff invariant curves can appear (as the one in Fig. 4) and even with more complicated shapes can appear. See [13] for details.

Just for fun we show in Fig. 5 an even wilder non-Birkhoff curve and a magnification. It appears for $\kappa = 0.6076$, very close to κ^*, starting at $(0, 1.145)$. Similar curves appear for very close initial

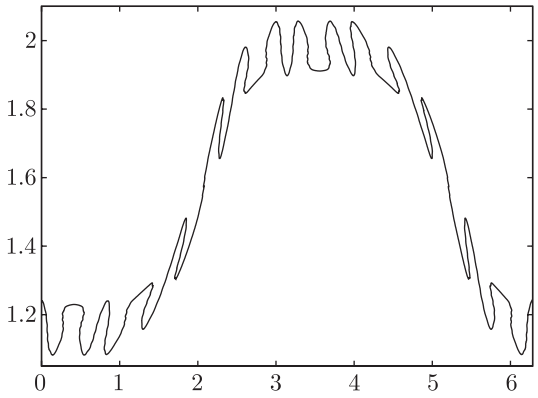

Fig. 4. A non-Birkhoff invariant curve for $\kappa = 0.56$. Points on the bottom of it and not too far belong to the chaotic zone associated to $(0, 0)$. Nearby points on the top belong to the chaotic zone associated to (π, π).

points. As a check, for both figures one has repeated the computation after transients larger than 3×10^9 for $\kappa = 0.56$ and larger than 6×10^9 for $\kappa = 0.6076$, with identical results.

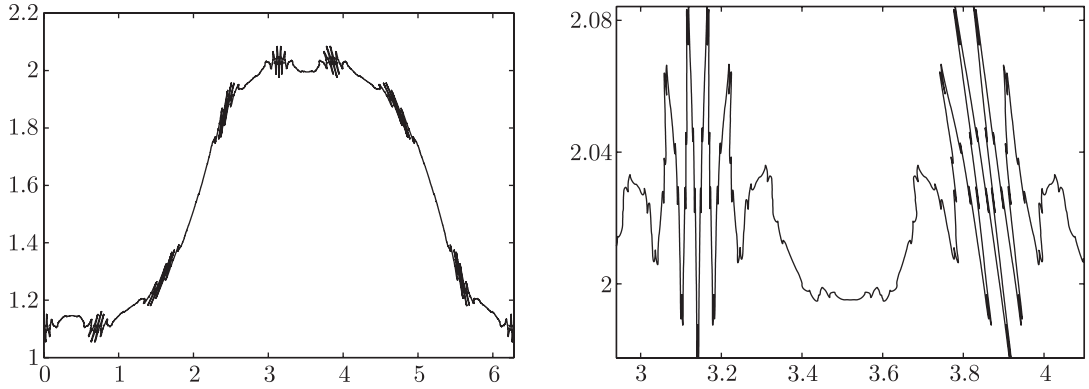

Fig. 5. A wild non-Birkhoff invariant curve for $\kappa = 0.6076$. The comments on the caption of Fig. 4 also apply. Left: global view. Right: a magnification.

Finally, we compute the maximal Lyapunov exponent, Λ, for (5.1) and how it evolves as a function of κ for κ between 0.01 and 1. The results are shown in Fig. 6. Typically one starts very close to $(0, 0)$. Every 10^6 iterations until 10^9 the log of the norm of the transported vector is stored. The Lyapunov exponent is estimated from the last value of the log of the norm and also using the slope of a fit. Both values are rather close for most of the values of κ. If the relative difference exceeds 1/30, one uses more initial points and one takes the average.

5.2. A Discrete Perturbation of the Initial Quasi-periodic Flow

We can consider a discrete version of the initial flow and perturb it so that the lines in the direction of the vector $(\omega, 1)$ are no longer invariant. To this end we use the map in $\mathbb{T}^2 = [-1/2, 1/2)^2$ defined by

$$P\begin{pmatrix} x \\ y \end{pmatrix} = \begin{pmatrix} \omega\varepsilon p_1(x,y) \\ \varepsilon p_2(x,y) \end{pmatrix}, \quad p_1(x,y) = \sin^2(\pi x) + \sin^2(\pi y), \quad p_2(x,y) = p_1(x,y) + \sin^3(\pi x)\cos(\pi x), \tag{5.4}$$

taking modulus 1 when we leave the domain. It is obvious that due to the inclusion of the last term in $p_2(x, y)$ the points do not move in the direction of $(\omega, 1)$. But taking into account that near the origin the dominant terms are the quadratic ones, both the contributions to the number of iterates

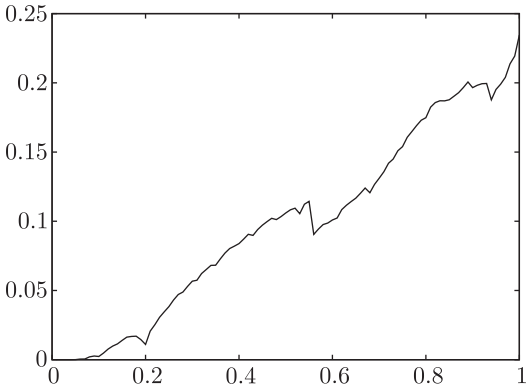

Fig. 6. Evolution of Λ for (5.1) as a function of κ. See the text for details.

and to the Lyapunov exponents of passages very close to $(0,0)$ are of the same type as the ones presented in Proposition 4.

As before, the origin is parabolic with an invariant manifold that has an unstable and a stable branch. To obtain an approximation of the manifold, we look for y as a formal expansion $y = g(x) = \sum_{i\geqslant 1} \alpha_i x^i$, asking for invariance. If we denote as $(\bar{x}, \bar{y})^T$ the image under P of $(x, y)^T$, we require $(\bar{x}, g(\bar{x}))^T = P((x, g(x))^T)$. It is elementary to obtain the coefficients α_i until the desired order.

For (5.4) one has taken as parameters $\omega =$ golden number and $\varepsilon = 0.1$. Using the expansion to order 9 and a fundamental domain $\mathcal{D}$ that in x goes from 0.01 to $0.0102219\ldots$, one can compute successive images of $\mathcal{D}$. Figure 7 shows some of these images, namely, $P^{260}(\mathcal{D})$, $P^{400}(\mathcal{D})$ and $P^{545}(\mathcal{D})$. Up to P^{260} the images reached 21 times either the upper or the right boundaries of $\mathbb{T}^2$ and all of them are very close to straight segments. For the successive iterates the images of $\mathcal{D}$ start to fold and later, being folded, are very close to a straight segment that folds again and again under iteration.

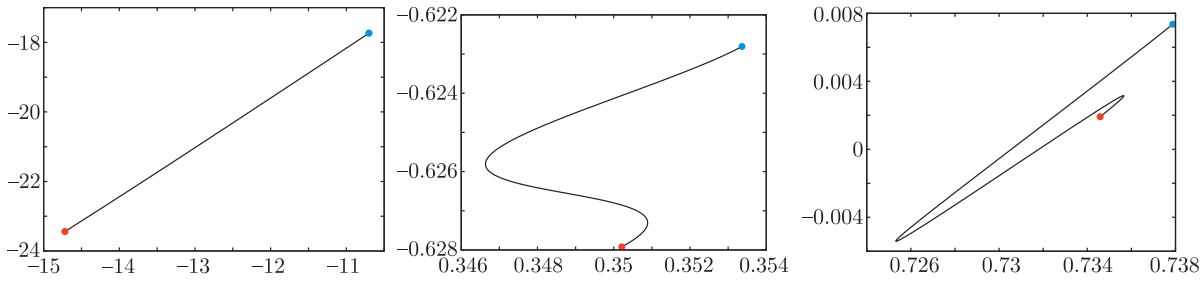

Fig. 7. Images of the fundamental domain $\mathcal{D}$ under 260, 400 and 545 iterations of P from left to right. For better visualization the values of the coordinates x, y have been multiplied by 100. In all the plots the image of the initial point in $\mathcal{D}$ is marked in red and that of the final point in blue.

Figure 8 shows, in a similar way, the image of the iterate P^{1000}, but for a better visualization of the folds of folds we plot the variables x and $y - 1.4x$.

These results give evidence that the phenomena for (5.4) are similar to the ones which appear in Section 5.1 due to homoclinic points. This gives rise to chaos and, in the present case, to a positive Lyapunov exponent.

To have evidence of this, we have taken 100 initial conditions with $y = 0$, $x = -0.495(0.01)0.495$ and we did 10^{12} iterates for each one, storing the log of the norm of the transported vector every 10^8 iterates. The Lyapunov exponent is estimated in two ways, as before. But now the values using the final value and the slope of the fit are not the main reason for the discrepancy. It turns out to be related to the different initial points.

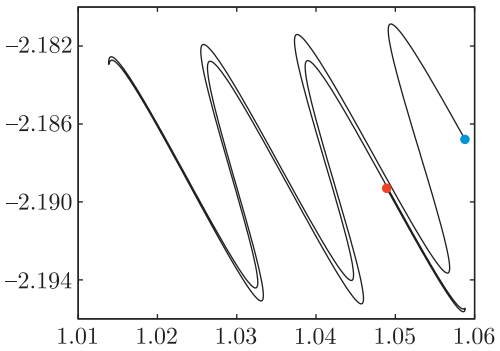

Fig. 8. Images of the fundamental domain $\mathcal{D}$ after 1000 iterations. See the text and the previous caption for details.

Using the average of the values computed for the 100 initial conditions, the relative differences are small, of the order of 0.01. Both are close to 4.9×10^{-4}, small but nonnegligible, as was the case with the maps in [9], where the values were below 10^{-9} and could be considered as irrelevant. The reason for the discrepancy, depending on the initial point, is how close to $(0, 0)$ come the successive iterates.

When the distance to the origin is small and is mainly dominated by the quadratic terms, one can use the bounds derived in Section 3 for $\gamma = 2$, denoting, as we did before, the minimal distance to the origin as u. Then the contribution to the number of iterates is of the order of u^{-1}, while the contribution to the norm of the transported vector is $\mathcal{O}(u^{-2})$. This gives a "local contribution" to the Lyapunov exponent of the order of $u \log(u)$, which is very small if u is small.

To check the passages near $(0, 0)$ in every simulation, we have checked when the minimal distance to the origin was achieved, for small values of this distance. The results, for the 100 points and 10^{12} iterates for each one of them, are that the minimal distances are below 10^m, for $m = 8$, 9, 10 and 11 in 14392, 1400, 141 and 13 cases, respectively. A more detailed information is shown in Fig. 9. It is not a surprise that, for some initial points for which a passage at distance $< 10^{-11}$ from the origin appears, it gives Lyapunov estimates of the order of one half of the average.

Furthermore, despite the lines of slope $1/\omega$ are not preserved, the approximate equidensity of passages through the minimal distance line is preserved, as the values above show. This is clearly seen in Fig. 9 until values of the minimal distance $\approx 10^{-11}$. Below this value there are very few cases.

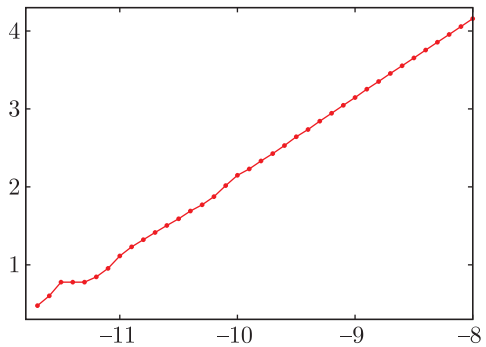

Fig. 9. Abundance of passages at minimal distance. The horizontal variable, say r, shows $\log_{10}$ of the minimal distance of the iterates to the origin. If there are m cases in which the minimal distance is below 10^r, the vertical variable is $\log_{10}(m)$.

5.3. Some Comments

From the previous examples we see that in the case of Section 5.1 there are parabolic fixed points which are topologically hyperbolic, with an unstable and a stable manifold, which despite the passage close to the fixed points produces a decreasing effect in the Lyapunov exponent. But this is not too relevant. Other truly hyperbolic objects (periodic orbits) play the role.

In Section 5.2 the parabolic fixed point is of different type: it has a unique invariant manifold with an unstable and a stable branch. In that case there are many passages very close to the fixed point and they play a stronger role in the decrease of the Lyapunov exponent. Furthermore, the estimates can differ by nonnegligible quantities depending on the initial point.

In systems with hyperbolic objects the passage close to them has a good contribution to the Lyapunov exponent. Later the contribution can decrease when passing through domains which reduce the contribution. A typical example appears in Hamiltonian systems if the orbit stays for a long time in the vicinity of a sticky torus.

As an old example, the classical Hénon attractor $(x, y) \mapsto (1 - ax^2 + y, bx)$ with $a = 1.4$, $b = 0.3$, the effect of the dominant eigenvalue λ_m at the upper hyperbolic point is $\log|\lambda_m| \approx 0.6542706$. Taking 100 initial points close to this hyperbolic point and doing 10^{10} iterates for each one, one obtains an average value $\Lambda \approx 0.419216$, which is almost identical for all of the points, with maximal differences of the order of 10^{-5}. The passages away from the fixed point play a small role.

6. CONCLUSIONS

We have presented some exceptional models that display chaos without any homoclinic or heteroclinic point. They are based on quasi-periodicity. Also, despite exhibiting chaotic dynamics, these models have zero maximal Lyapunov exponents. This can lead to asking for measures of weak chaoticity. The models have been shown to change to positive Lyapunov exponent under higher-order perturbations or in the case of some quite exceptional frequencies. Related topics, as the effect of different types of parabolic points, have also been considered.

ACKNOWLEDGMENTS

Thanks to J. Timoneda for maintaining the computing facilities of the Dynamical Systems Group of the Universitat de Barcelona, which have been largely used in this work to make many simulations.

FUNDING

This work has been supported by grants MTM2016-80117-P (Spain) and 2017-SGR-1374 (Catalonia).

CONFLICT OF INTEREST

The authors declare that they have no conflicts of interest.

REFERENCES

1. Aulbach, B. and Kieninger, B., On Three Definitions of Chaos, *Nonlinear Dyn. Syst. Theory,* 2001, vol. 1, no. 1, pp. 23–37.
2. Chirikov, B. V., A Universal Instability of Many-Dimensional Oscillator Systems, *Phys. Rep.,* 1979, vol. 52, no. 5, pp. 263–379.
3. Danforth, C. M., Chaos in an Atmosphere Hanging on a Wall, http://mpe.dimacs.rutgers.edu/2013/03/17/chaos-in-an-atmosphere-hanging-on-a-wall/ (Mathematics of Planet Earth, 2013).
4. Devaney, R. L., *An Introduction to Chaotic Dynamical Systems,* 2nd ed., New York: Addison-Wesley, 1989.
5. Fontich, E., Simó, C., and Vieiro, A., On the "Hidden" Harmonics Associated to Best Approximants due to Quasi-Periodicity in Splitting Phenomena, *Regul. Chaotic Dyn.,* 2018, vol. 23, no. 6, pp. 638–653.
6. Garrido, L. and Simó, C., Some Ideas about Strange Attractors, in *Dynamical Systems and Chaos (Sitges/Barcelona, 1982),* Lecture Notes in Phys., vol. 179, Berlin: Springer, 1983, pp. 1–28.
7. Khinchin, A. Ya., *Continued Fractions,* Chicago, Ill.: Univ. of Chicago, 1964.
8. Kozlov, V. V., Closed Orbits and Chaotic Dynamics of a Charged Particle in a Periodic Electromagnetic Field, *Regul. Chaotic Dyn.,* 1997, vol. 2, no. 1, pp. 3–12.
9. Martínez, R. and Simó, C., A Simple Family of Exceptional Maps with Chaotic Behavior, *Qual. Theory Dyn. Syst.,* 2020, vol. 19, no. 1, Art. 40, 14 pp.
10. Marqués, D. and Schleischitz, J., On a Problem Posed by Mahler, *J. Aust. Math. Soc.,* 2016, vol. 100, no. 1, pp. 86–107.
11. Poincaré, H., *Les méthodes nouvelles de la mécanique céleste: In 3 Vols.,* Paris: Gauthier-Villars, 1892, 1899.
12. Sander, E. and Yorke, J. A., The Many Facets of Chaos, *Internat. J. Bifur. Chaos Appl. Sci. Engrg.,* 2015, vol. 25, no. 4, 1530011, 15 pp.
13. Simó, C., Invariant Curves of Perturbations of Non-Twist Integrable Area Preserving Maps, *Regul. Chaotic Dyn.,* 1998, vol. 3, no. 3, pp. 180–195.